文章编号：0258-7025(2009)12-3125-08

Laser Assisted Fabrication for Controlled Single-Walled Carbon Nanotube Synthesis and Processing

(Invited Paper)

W. Xiong Y. Gao M. Mahjouri-Samani Y. S. Zhou
M. Mitchell J. B. Park Y. F. Lu*

(*Department of Electrical Engineering, University of Nebraska-Lincoln, Lincoln, NE* 68588-0511, *USA*)

* *Corresponding author*: *ylu2@unl.edu*

Received October 13, 2009

Abstract Although significant progress has been made in large scale and high quality single-walled carbon nanotube (SWNT) synthesis, the fabrication of SWNT-based functional devices still faces many challenges due to the lack of good methods to precisely control over SWNTs growth location, orientation, alignment, and electronic properties. Hence, development of practical methods for well-controlled SWNT-based device fabrication has drawn great interests from both academics and industry. Due to numerous advantages, laser-based techniques are applied in controlled fabrication of SWNT devices. In this paper, we first introduce the laser assisted chemical vapor deposition (LCVD) process, and then different aspects of controllability in device fabrication are described in three sections: 1) location and orientation control of SWNT channels integration using optical near-field effects; 2) alignment control of SWNTs arrays using electrical biasing polarities; 3) SWNTs electronic property control using laser-induced breakdown technique. Our experimental results show that well-organized individual SWNT channels or arrays with location, orientation, alignment, and electronic property control can be achieved through laser assisted fabrication process, which is a promising solution for the fabrication of future SWNT-based devices.

Key words single-walled carbon nanotubes; laser-assisted chemical vapor deposition; location and orientation control; alignment control; electronic property control

CLCN: V261.8 **Document Code**: A **doi**: 10.3788/CJL20093612.3125

1 Introduction

Due to numerous superior properties unparalleled by most known materials, carbon nanotubes (CNTs) are regarded as one of the most important materials in modern nanotechnology. Since the discovery of CNTs in 1991[1], these tiny tubes show great potential in various applications, such as nano-probes[2], displays[3], sensors[4], energy-storage media[5], and molecular electronics[6]. Significant progress has been made in the carbon nanotube synthesis with three well-established methods: arc discharge[7], laser ablation[8], and chemical vapor deposition (CVD)[9].

However, there is still a big gap between high efficient single-walled carbon nanotube (SWNT) synthesis and fabrication of SWNT-based devices. The main challenges are the lack of control in the synthesis and processing of SWNTs. For example, the location and orientation control on large substrates, which is needed for the scalable production of nanotube electronics and other devices; the alignment control of SWNT arrays, which is needed for different device applications where either horizontally or vertically aligned SWNT forest structures are desired; and the electronic property control that determines whether a nanotube is metallic or semiconducting. In order to address these challenges, laser techniques are applied, since they could provide further controllability over SWNT synthesis and processing.

In this paper, we will first introduce the laser assisted CVD (LCVD) process for SWNT synthesis. Then we will demonstrate our recent work on controlled synthesis and processing using LCVD as following: 1) location and orientation control of SWNT channels integration using optical near-field effects; 2) alignment control of SWNTs arrays using electrical biasing polarities; 3) SWNTs electronic property control using laser-induced breakdown technique. The results show that LCVD with

Supported by the National Science Foundation for the financial support under Grant Nos. ECCS 0621899 and ECCS 0652905.

the aid of post-growth laser processing can successfully realize the simultaneous integration of well-controlled SWNT connections between predefined electrodes, alignment control of SWNT arrays in vertical and horizontal directions, and SWNTs electronic property control. Although more work is still required to improve the efficiency of controlled SWNT synthesis and processing, laser assisted fabrication technique clearly exhibits its potential for the future SWNT-based device fabrication.

2 LCVD

In general, the LCVD technique for carbon nanotube growth uses lasers as the thermal source for catalytic thermal decomposition of carbon species to form single-wall or multi-walled carbon nanotubes on various substrates. It has provided several unique advantages over the conventional CVD process. For instance, it has a much shorter heating and cooling cycle for the entire process[10,11] and the capability of localized processing[12]. Furthermore, its inherent and unique secondary effects of laser interaction with matters such as optical near-field enhancements[13] and resonant absorption[14] offer it further controllability on synthesis location, orientation, and even chirality[14] of SWNTs during LCVD process.

The conventional schematic diagrams of the LCVD process for SWNT field-effect transistor (FET) fabrication and corresponding system are shown in Fig. 1. Heavily doped Si wafers covered with a 2-μm-thick SiO_2 layer were used as the substrates. The electrode patterns were fabricated by conventional photolithography followed by direct current (DC) sputtering. 200-nm thick Ruthenium (Ru) and 2-nm thick iron (Fe) films were deposited sequentially on the SiO_2 surface. Ru was used as the electrode material because of its low solubility with Fe, high work function, and high melting point. The Fe thin film was used as the catalyst for SWNT growth. Growth of SWNTs was carried out in an LCVD chamber, as shown in Fig. 1. A continuous-wave (CW) CO_2 laser (Synrad, firestar v40, wavelength = 10.6 μm, laser beam diameter = 2.5 ± 0.5 mm) was used to irradiate the patterned substrates. The laser power was adjusted to maintain a stable substrate temperature. Typical laser power used was ranged from 10 to 20 W. A DC voltage was applied between the electrodes to assist the self-aligned growth of SWNTs. The magnitude of the DC bias varied according to the gap width, with typical values of 1～1.5 V/μm. A gas mixture of acetylene (C_2H_2) and anhydrous ammonia (NH_3) with a volume ratio of 1∶10 was introduced into the chamber. Anhydrous ammonia was used as a buffer gas in the LCVD process to dilute acetylene, create an etching environment to suppress the growth of amorphous carbon, and protect catalyst particles from being poisoned by amorphous carbon[15]. The reaction pressure was maintained at 10 Torr. The growth temperature of SWNTs was controlled at ～700 ℃. A multi-meter was used to detect the current flow in the circuit when SWNTs bridged electrodes, which enabled in-situ monitoring of the growth condition and detection of the end-point of the process. The reaction process was terminated immediately when a SWNT bridge structure was formed.

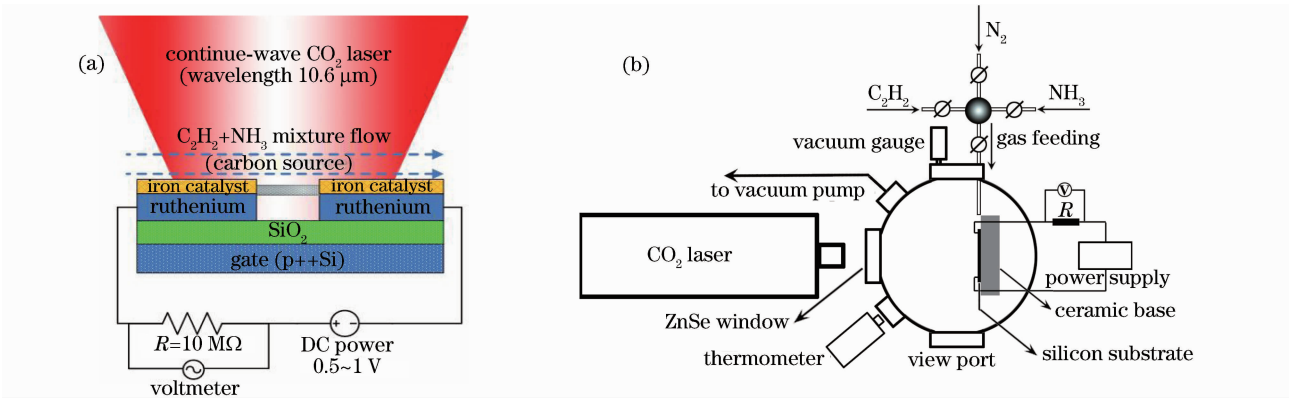

Fig. 1 (a) Conventional LCVD process for SWNT-FET fabrication and (b) schematic of corresponding LCVD system

For SWNT characterization, a field-emission scanning electron microscope (Hitachi S4700 FE-SEM, maximum resolution of 1.2 nm at 25 kV) was used to see the morphological structures of SWNT devices. A Renishaw inVia dispersive micro-Raman spectrometer was used for Raman spectro-

scopic study. A standard 50× objective lens was used for the Raman measurements, which provided a focal spot diameter of 2 μm and a power density of 2550 W/cm^2. An argon-ion laser operated at 488 nm was used as the excitation source for the Raman measurements.

Figure 2(a) shows a typical scanning electronic microscope (SEM) image of the multi-SWNT bridging structures. Figure 2(b) shows a typical Raman spectrum of the SWNTs. A sharp radial breathing mode (RBM) peak at 166.3 cm^{-1} demonstrates the formation of the SWNTs with a diameter around 1.5 nm (for isolated SWNT, the diameter $d_t = 248/\omega_{RBM}$[16]). The multi-SWNT bridging structures provide stable platforms for SWNT-based sensors. However, as we can see, the position and orientation had not been precisely controlled by using the parallel electrodes. Such structures are also not suitable for highly sensitive detection at single molecular scale, since their performances are determined by the collective contribution of all connected SWNTs. Therefore, single-SWNT bridging structure was suggested.

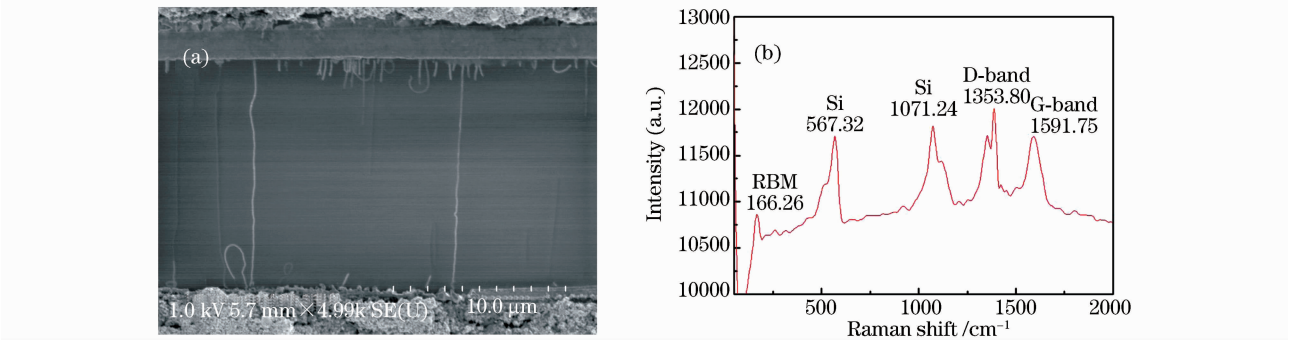

Fig. 2 (a) Typical SEM image of the multi-SWNT bridging structure and (b) typical Raman spectrum of the SWNTs

3 Location and Orientation Control of SWNT Channels Integration Using Optical Near-Field Effects

Although the conventional LCVD process could successfully fabricate the SWNT bridging structures, the control over SWNT growth site and orientation was still poor. Besides, the relatively high substrate temperature (700 ℃) for SWNTs synthesis not only makes the fabrication process costly but also blocks its applications with many other fabrication process which can only sustain limited temperature. For example, present back-end complementary metal oxide semiconductor (CMOS) technology allows a maximum process temperature of 400～450 ℃, the limit being set by the mechanical integrity of low dielectric constant intermetal dielectrics[17]. In order to solve the above problems, we introduce a novel laser-based strategy for precisely controlled SWNT-growth at a relatively low substrate temperature using optical near-field effects. According to the experimental results and numerical simulations, the laser-induced optical near-field effects can produce nanoscale localized heating at electrode tips, which stimulates the SWNT growth right at the tips. Two obvious advantages are observed for this technique: precise placement control of SWNT bridges and low substrate temperature process.

Figure 3 shows the schematic setup for the fabrication of single-SWNT bridging structures. The LCVD process described in the previous section was used. In addition, sharp electrode tips were formed by focused ion beam (FIB) nano-machining using an FEI Strata 200xp system. The electrode gap distance was controlled around 200 nm. The purpose of making sharp electrode tips is to produce enhanced optical near-field under the laser beam to stimulate the SWNT growth at the tip apex. Due to the optical near-field heat enhancement, the substrate temperature of the LCVD process was only 500 ℃, which is 200 ℃ lower than the conventional LCVD process.

Figure 4(a) shows a typical SEM image of the metallic electrode for electrical contact. Figure 4 (b) shows the enlarged image of the circled area in Fig. 4(a). An SWNT is clearly observed to bridge the electrode pair. The length of the SWNT was determined by the electrode gap distance. The SWNT showed a small-amplitude vibration under the electron beam irradiation, which contributed to the appeared large diameter. Sharp contrast between the SWNT and the underneath substrate indicates that the SWNT is suspended above the SiO_2

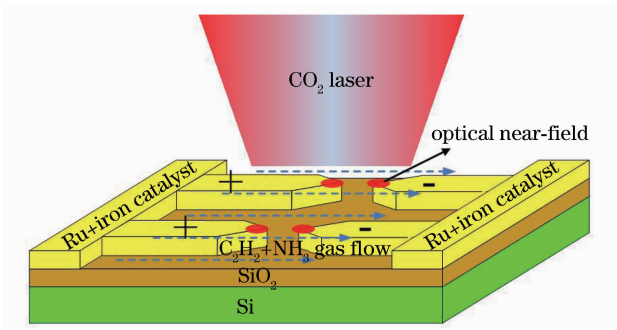

Fig. 3 Illustration of LCVD for self-aligned growth of single-SWNT bridging structures using optical near-field effects

surface[18].

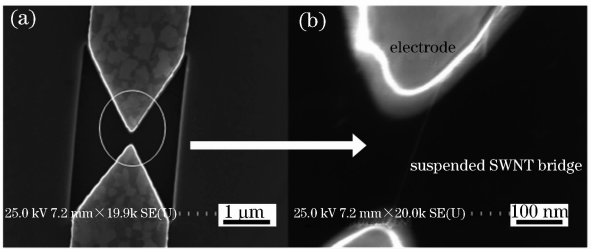

Fig. 4 SEM images of (a) electrodes and (b) individual SWNT bridge structure

It is known that ultra-sharp metallic tips can be used as optical antennae to localize and enhance optical fields[19,20]. Furthermore, the optical near-field effects result in enhanced eddy-currents and localized nanoscale heating at the metallic tips. Numerical simulations have been carried out to evaluate the contribution of the optical near-field effects in the SWNT growth process using the high frequency structure simulator (HFSS, Ansoft) software package. The incident laser beam was assumed to be linearly polarized and propagating perpendicularly to the substrate surface. The electromagnetic frequency was 28.3 THz, equivalent to the CO_2 laser wavelength (10.6 μm) used in the LCVD process, and the tip radius was assumed to be 20 nm. Figure 5(a) shows the simulation results of the electric field in the metallic tips. Significant electric field enhancement can be observed at the localized tip areas, almost ten times higher than that of the rest of the electrodes. Since the electromagnetic field generates eddy currents, the enhanced high-frequency electric field at the tips results in significantly enhanced local eddy currents and yields an enhanced localized heating at nanometer scales. Figure 5(b) shows the heat distribution on the surface of the electrode tips. The localized heating enhancement reaches the maximum value at the tips,

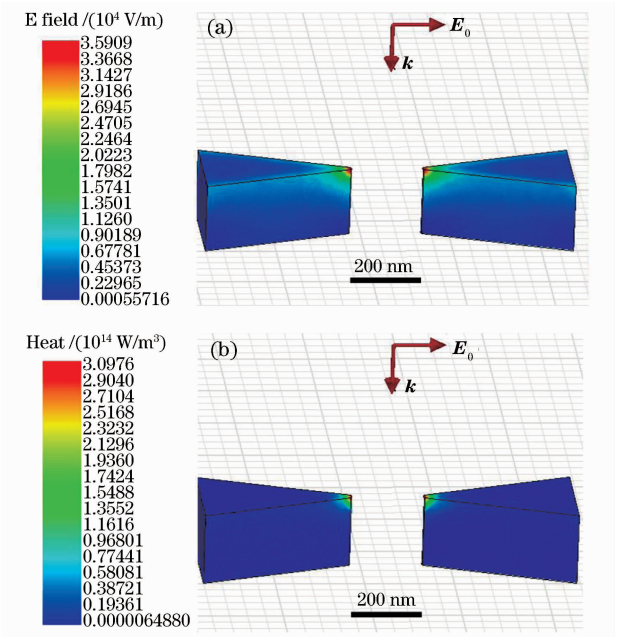

Fig. 5 Numerical simulation results of (a) electric field and (b) heat distributions around ruthenium tips

over ten times higher than that of the rest of the electrodes. Therefore, a significant temperature increase at the tips is induced by the optical near-field effects. Since the SWNT growth strongly depends on the reaction temperature[21], an increased temperature at metallic tips will significantly promote the growth of SWNTs at the tips compared with the rest part of the electrodes, which can explain the preferential growth of SWNTs at the tips. In addition, a significant temperature increase at metallic tips also benefits the stable SWNT-metal adhesion due to the formation of carbide at high temperature, which promises stable SWNT-bridge structures.

In summary, a novel laser-based method for highly controlled growth of suspended SWNT channels using optical near-field effects was developed. Laser induced near-field enhancements produce nanoscale localized heating at the electrode tips, which stimulated and confined the SWNT growth at the tips. Precise location and orientation control, low substrate temperature, and reliable SWNT/metal contact were achieved by this laser-based optical near-field driven method.

4 Alignment Control of SWNT Arrays Using Different Bias Polarities

Alignment control of SWNT arrays synthesis on metallic electrodes was also studied by applying

electrical biases of different polarities during LCVD process. As shown in Fig.6(a), densely packed SWNTs were observed on both the anode and cathode. Surface-bounded SWNTs were observed on the anode sticking out from the electrode and crawling on the SiO_2 surface. A fuzzy edge was observed for the anode. However, vertically aligned SWNTs were observed on the cathode. A neat and clean edge was observed for the cathode. Raman spectra were measured on the anode and cathode separately, as shown in Figs.6(b) and (c). The RBM signals ranging from 100 to 300 cm^{-1}, D- and G-bands were observed on both electrodes. The signal observed around 1000 cm^{-1} was the Si background signal. The Raman spectrum from the anode shows a stronger RBM intensity while the spectrum from cathode shows stronger D- and G-band intensities. The difference of the Raman spectra was ascribed to the different alignments of the SWNTs on the electrodes. The surface crawling SWNTs on the anode have large Raman scattering cross-sections. Therefore, stronger RBM signals were observed in Fig.6(b). Vertically aligned SWNTs (with end caps exposing to the surface) on the cathode have small Raman scattering cross-sections which lead to weak RBM peaks. The stronger D- and G-bands indicate more carbon deposition, as shown in Fig.6(c).

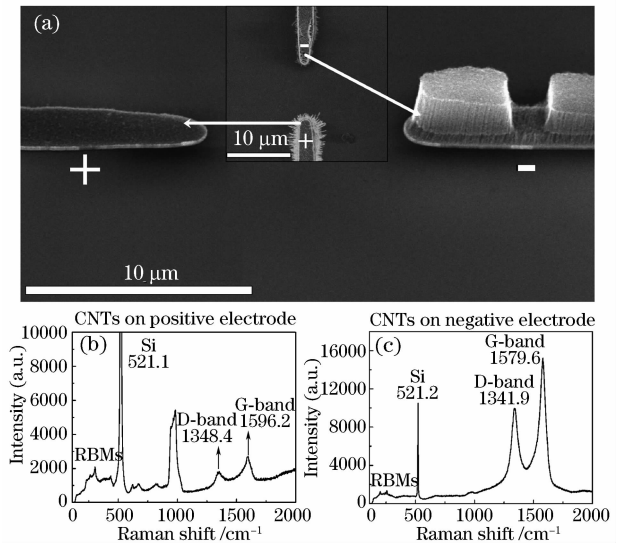

Fig.6 (a) A typical SEM image of SWNTs with different alignments grown on the positively and negatively charged electrodes. Typical Raman spectra of SWNTs grown on (b) a positive electrode and (c) a negative electrode

It was suggested that the movement of catalyst nanoparticles (NPs) was responsible for the CNT alignment. As shown in the inset of Fig.7(a), surface crawling CNTs have bright spots at their ends, which are the catalyst NPs. In Fig.7(b), a shiny top layer was observed for the vertically aligned CNT arrays, which indicated the coalesced catalyst NPs. Therefore, a tip-growth mode is suggested for the CNT growth in the LCVD process. The catalyst NPs, iron nanoparticles, are suggested to be positively charged due to the relatively stronger electron affinity of carbon. Iron has a work function of 4.67 eV[22], while an average work function of CNTs was calculated to be 5.44 eV[23,24]. Therefore, CNTs have a stronger electron affinity than iron NPs and attract electrons from the iron atoms, making the iron NPs positively charged. As a result, the catalyst NPs at the anode are repulsed by the positively charged electrodes and move away from the positive electrodes towards the negatively charged electrodes following the directions of the electric field. It is well known that CNTs nucleate and grow from carbon-saturated catalyst NPs. Therefore, growth of CNTs follows the moving tracks of the catalyst NPs. For the CNTs grown on the negatively charged electrodes, vertically aligned CNTs were ascribed to the joint contribution from following interactions. The first was the van der Waals interaction among the CNTs, which made high density CNT arrays entangled and vertically aligned. The second was the attractive force be-

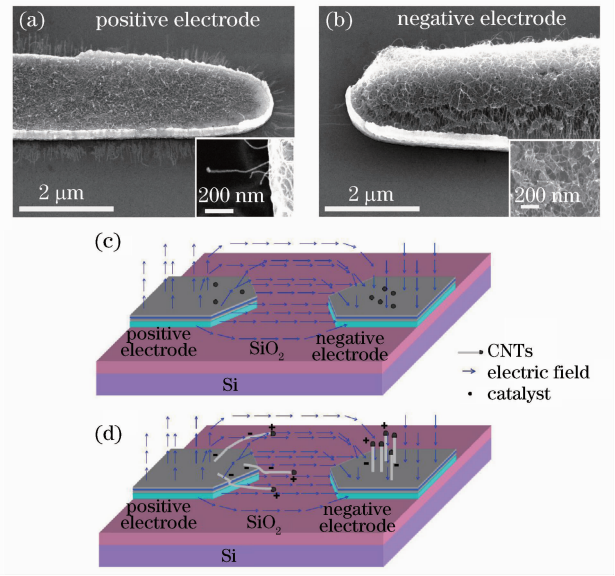

Fig.7 SEM images of CNTs on the (a) positive and (b) negative electrodes, respectively; (c) and (d) are schematics of CNT growth induced by the movement of positively charged catalyst NPs in the external electric field

tween the positively charged catalyst NPs and the negatively charged electrodes, which prevented CNTs from stretching outside. The third was the repulsing forces caused by the continuous growth of CNTs, which kept pushing the catalyst NPs outward. Therefore, the catalyst NPs were forced to move outside of the surface plane and induced vertically aligned growth of CNTs. It should be pointed out that there are also several other parameters influencing the movement of the catalyst NPs, including gas flow, thermal fluctuation, convection, van der Waals force, and physical barriers.

In summary, controllable growth of SWNTs with different alignments was achieved by applying biasing voltages of different polarities on the metallic electrodes. Horizontally and vertically aligned SWNT arrays were selectively grown on anode and cathode, respectively. The growth alignment control was ascribed to the movement of positively charged catalyst NPs under the static electric field.

5 Electric Property Control of SWNTs Using Laser Induced Breakdown Technique

Property control of SWNTs synthesized by LCVD process was studied using laser induced breakdown method. Metallic-SWNTs (M-SWNTs) were selectively removed from surface bounded SWNT mixtures through well-tuned laser irradiation process. Figure 8 shows the schematic of the experimental procedure. By using the LCVD method, both well-aligned SWNTs between parallel electrodes and randomly distributed SWNT mixtures were prepared. M-SWNTs were then selectively heated and removed by optical parametric oscillator (OPO) laser irradiation.

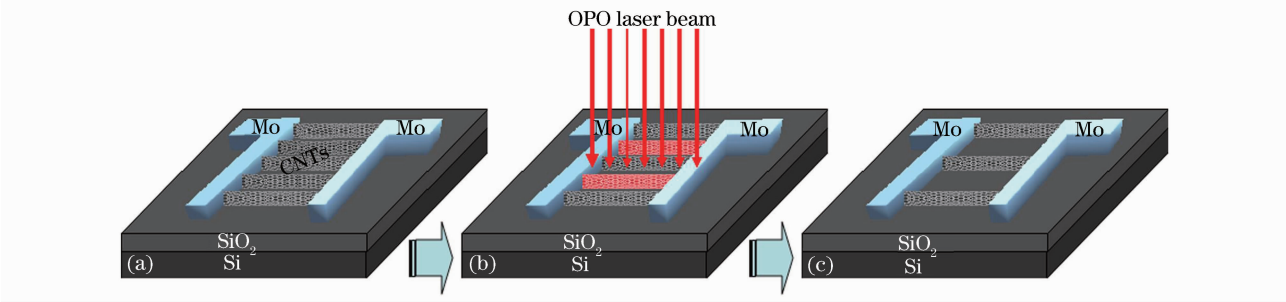

Fig. 8 Schematic of the experimental process. (a) SWNT array before laser irradiation; (b) laser irradiation process to remove m-SWNTs; (c) semiconducting-SWNTs (s-SWNTs) array after laser irradiation

An OPO wavelength-tunable laser (Continuum, Panther EX) was used as a source, which provides laser irradiation with wavelengths ranging from 215 to 2550 nm. Pulsed laser beams with a wavelength of 2 μm were used for the selective removal process. It is suggested that laser beams of longer wavelengths would be also possible as long as the threshold power is satisfied. However, due to the sharp drop of the output power for wavelength over 2 μm in our existing OPO tunable laser, we did not investigate the wavelength larger than 2 μm. Laser beams of shorter wavelengths could cause obvious damages to both s- and m-SWNTs due to the high energy photons. The OPO laser provided laser pulses with pulse duration of 6 ns at a frequency of 10 Hz. The energy of each pulse was about 3 mJ. A lens with 50 mm focal length was used to control the spot size and the laser fluence irradiated on the samples. The diameter of the laser spots on samples was controlled around 1.5 mm. Therefore, the power density was estimated to be 1.8 MW/mm^2.

To evaluate the effects of the selective removal of metallic tubes, I-V characterization of the SWNT devices was carried out before and after laser irradiation. Figures 9(a) and (b) show the I_d-V_g and I_d-V_{ds} curves of a CNT array before laser irradiation. The results confirm the existence of metallic tubes due to the curve's linearity, high constant current value, and absence of V_g dependence. Figures 9(c) and (d) show the I_d-V_g and I_d-V_{ds} curves of the same samples after the laser irradiation. In contrast to the I-V characteristics measured before laser irradiation, the I-V curves show nonlinear semiconducting behavior, clear V_g dependence, and obviously reduced current, which indicate the successful removal of the metallic tubes after OPO laser irradiation. Furthermore, the comparison of Raman spectra of the CNT mixtures in various areas with different laser irradiation intensity also indicated the selective removal of metallic tubes. Figure 10 shows the Raman spectra from three different spots on the sample , corresponding to the SEM

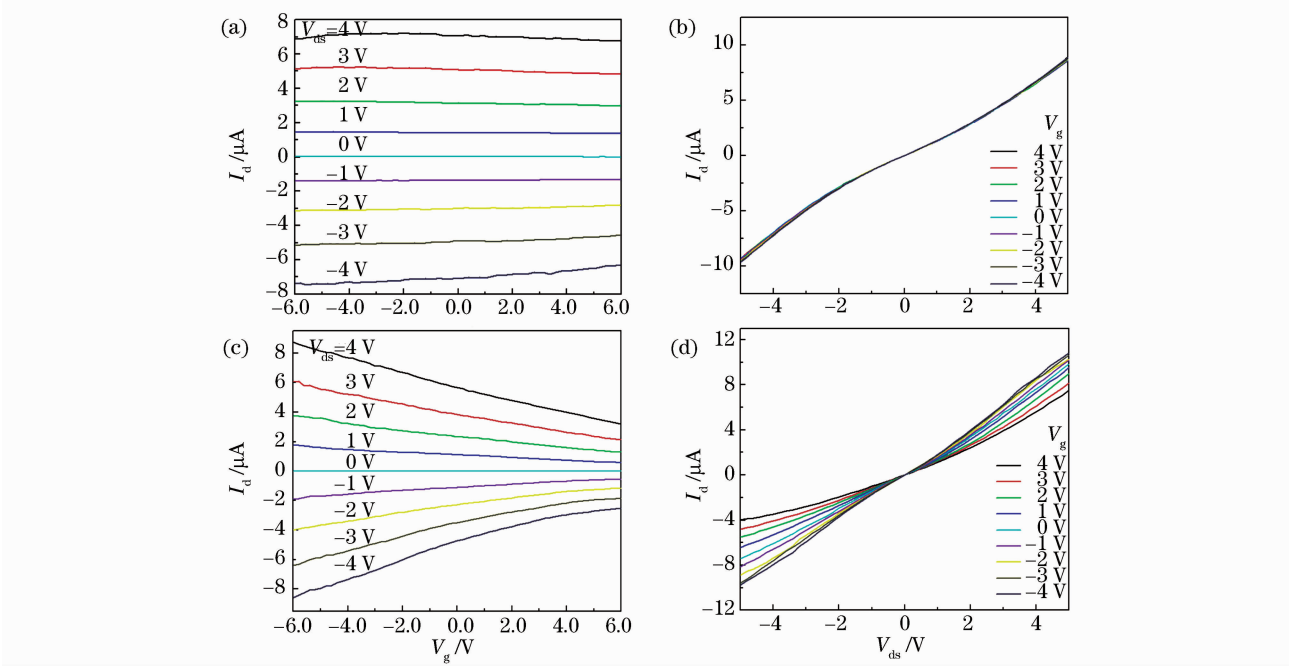

Fig. 9　I_d-V_g and I_d-V_{ds} curves of the original sample (a), (b) before and (c), (d) after laser irradiation respectively, with laser wavelength of 2 μm and irradiation duration of 20 s

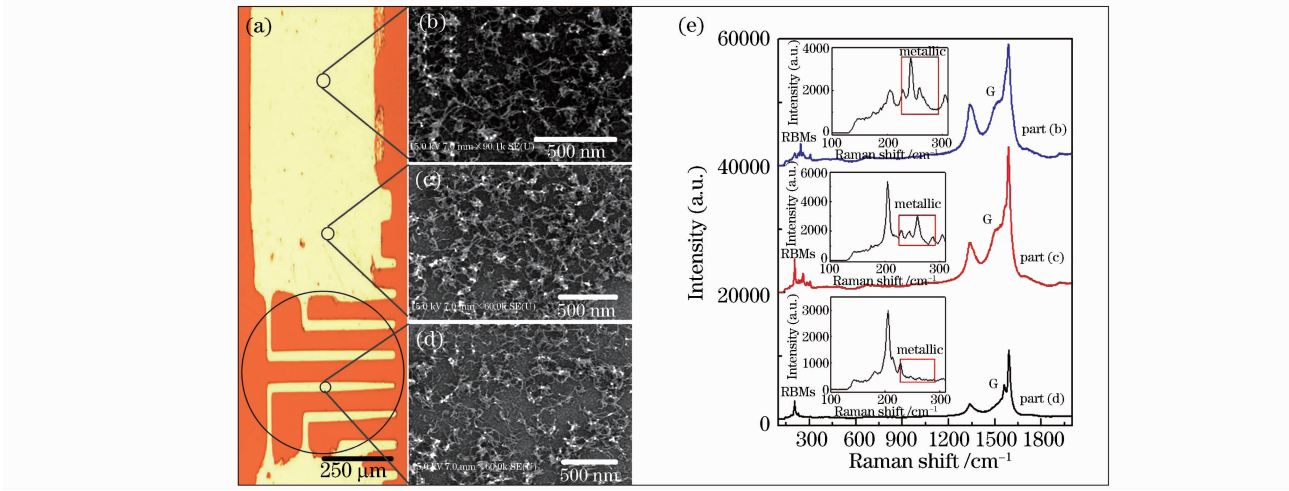

Fig. 10　(a) Optical image of the electrode with a circle indicating the OPO laser spot; (b), (c), and (d) SEM images of the SWNTs on the electrode away from the corresponding laser spots. (e) Raman spectra obtained from different parts of the electrode corresponding to each SEM pictures. The insets are the close up view of RBM peaks for each spectrum. The G-band Lorentzian line shape with no metallic RBM peak is observed in the region of the laser spot. The BWF line shape line shape and metallic RBM peaks are observed away from the laser spot

images, starting from the OPO laser spot and moving away from it. In the OPO laser spot, G-band shows Lorentzian line shape indicating the existence of only s-SWNTs in this region. In the region away from the OPO laser spot, the G-band turns into Berit-Wigner-Fano (BWF) line shape indicating the existence of m-SWNTs[25]. Besides, RBM peaks were also analyzed to determine the nanotube chiralities and therefore the types of the single-walled carbon nanotubes existed in the samples. According to the Kataura Plot[26,27], the RBMs between 225 and 290 cm^{-1} come from m-SWNTs due to their resonance with the 488-nm laser beam. The insets in the Fig. 10(e) show zoomed views of the RBM signals from different area of the sample corresponding to the SEM pictures. RBM signals coming from m-SWNTs (in the red boxes) are observed in the regions, which were not irradiated by the laser beams. Only RBM peaks arising from s-SWNTs were observed within the laser irradiated

region indicating the selective removal of m-SWNTs.

In summary, electronic property control of SWNTs was realized by selective removal of m-SWNTs from SWNT mixtures using laser-induced breakdown method. Optical near-field effects and free electron movement caused by the laser irradiation contributed to the selective heating and removal of m-SWNTs in open air.

6 Conclusion

The laser strategy for SWNT CVD synthesis and processing was discussed in this paper. Three aspects of controllability in laser assisted SWNT fabrication were demonstrated, i.e., growth location and orientation control, alignment control, and electronic property control. Thanks to several advantages of laser processing, the laser assisted fabrication opened up new routes for controlled SWNT synthesis and integration. Although the laser assisted SWNT fabrication is still in its initial stage, it is clear that future developments in nanotube-based science and technology will continue to rely on the further improved controlled synthesis of CNTs and the laser assisted fabrication techniques possess a great potential in future SWNT-based device fabrication.

References

1 S. Iijima. Helical microtubules of graphitic carbon [J]. *Nature*, 1991, **354**:56～58

2 H. Dai, J. H. Hafner, A. G. Rinzler *et al*.. Nanotubes as nanoprobes in scanning probe microscopy [J]. *Nature*, 1996, **384**(6605):147～150

3 W. B. Choi, D. S. Chung, J. H. Kang *et al*.. Fully sealed, high-brightness carbon-nanotube field-emission display [J]. *Appl. Phys. Lett.*, 1999, **75**(20):3129～3131

4 J. Li, Y. Lu, Q. Ye *et al*.. Carbon nanotube sensors for gas and organic vapor detection [J]. *Nano Lett.*, 2003, **3**(7):929～933

5 G. Che, B. B. Lakshmi, E. R. Fisher *et al*.. Carbon nanotubule membranes for electrochemical energy storage and production [J]. *Nature*, 1998, **393**:346～349

6 S. J. Tans, A. R. M. Verschueren, C. Dekker. Room-temperature transistor based on a single carbon nanotube [J]. *Nature*, 1998, **393**(6680):49～52

7 C. Journet, W. K. Maser. Large-scale productionof single-walledcarbon nanotubesby the electric-arc technique [J]. *Nature*, 1997, **388**(6644):756～758

8 M. Yudasaka, T. Komatsu, T. Ichihashi *et al*.. Single-wall carbon nanotube formation by laser ablation using double-targets of carbon and metal [J]. *Chem. Phys. Lett.*, 1997, **278**(1-3):102～106

9 C. Bower, O. Zhou, W. Zhu *et al*.. Nucleation and growth of carbon nanotubes by microwave plasma chemical vapor deposition [J]. *Appl. Phys. Lett.*, 2000, **77**(17):2767～2769

10 J. Shi, Y. F. Lu, H. Wang *et al*.. Synthesis of suspended carbon nanotubes on silicon inverse-opal structures by laser-assisted chemical vapor deposition [J]. *Nanotechnology*, 2006, **17**(15):3822～3826

11 J. B. Park, S. H. Jeong, M. S. Jeong *et al*.. The rapid growth of vertically aligned carbon nanotubes using laser heating [J]. *Nanotechnology*, 2009, **20**(18):185604

12 J. B. Park, M. S. Jeong, S. H. Jeong. Direct writing of carbon nanotube patterns by laser-induced chemical vapor deposition on a transparent substrate [J]. *Appl. Surf. Sci.*, 2009, **255**(8):4526～4530

13 W. Xiong, Y. S. Zhou, M. Mahjouri-Samani *et al*.. Self-aligned growth of single-walled carbon nanotubes using optical near-field effects [J]. *Nanotechnology*, 2009, **20**(2):025601

14 K. Maehashi, Y. Ohno, K. Inoue *et al*.. Laser-resonance chirality selection in single-walled carbon nanotubes [C]. *ICPS-27. AIP Conference Proceedings*, 2005, **772**:1023～1024

15 T. K. Jang, J. H. Ahn, Y. H. Lee *et al*.. Effect of NH_3 and thickness of catalyst on growth of carbon nanotubes using thermal chemical vapor deposition [J]. *Chem. Phys. Lett.*, 2003, **372**(5-6):745～749

16 M. S. Dresselhaus, G. Dresselhaus, R. Saito *et al*.. Raman spectroscopy of carbon nanotubes [J]. *Phys. Rep.*, 2005, **409**(2):47～99

17 M. Morgen, E. T. Ryan, J. H. Zhao *et al*.. Low dielectric constant materials for ULSI interconnects [J]. *Annu. Rev. Mater. Sci.*, 2000, **30**:645～680

18 Y. Homma, S. Suzuki, Y. Kobayashi *et al*.. Mechanism of bright selective imaging of single-walled carbon nanotubes on insulators by scanning electron microscopy [J]. *Appl. Phys. Lett.*, 2004, **84**(10):1750～1752

19 N. Hayazawa, T. Yano, H. Watanabe *et al*.. Detection of an individual single-wall carbon nanotube by tip-enhanced near-field Raman spectroscopy [J]. *Chem. Phys. Lett.*, 2003, **376**(1-2):174～180

20 L. Novotny, R. X. Bian, X. S. Xie. Theory of nanometric optical tweezers [J]. *Phys. Rev. Lett.*, 1997, **79**(4):645～648

21 Y. G. Yao, Q. W. Li, J. Zhang *et al*.. emperature-mediated growth of single-walled carbon-nanotube intramolecular junctions [J]. *Nat. Mater.*, 2007, **6**(4):293～296

22 D. R. Lide. CRC Handbook of Chemistry and Physics [M]. 85th edition. Boca Raton: CRC Press, 2004

23 G. Zhou, W. Duan, B. Gu. Electronic structure and field-emission characteristics of open-ended single-walled carbon nanotubes [J]. *Phys. Rev. Lett.*, 2001, **87**(9):095504

24 Q. K. Yu, G. T. Qin, H. Li *et al*.. Mechanism of horizontally aligned growth of single-wall carbon nanotubes on R-plane sapphire [J]. *J. Phys. Chem. B*, 2006, **110**(45):22676～22680

25 S. D. M. Brown, A. Jorio, P. Corio *et al*.. Origin of the breit-wigner-fano lineshape of the tangential G-band feature of metallic carbon nanotubes [J]. *Phys. Rev. B*, 2001, **63**(15):155414

26 H. Kataura, Y. Kumazawa, Y. Maniwa *et al*.. Optical properties of single-wall carbon nanotubes [J]. *Synth. Met.*, 1999, **103**(1-3):2555～2558

27 R. Satio, G. Dresselhaus, M. S. Dresselhaus. Trigonal warping effect of carbon nanotubes [J]. *Phys. Rev. B*, 2000, **61**(4):2981～2990